On the reliability of the color gradient vector argument approach.

Belén Prados-Suarez[1] Pilar Sobrevilla[2] Eduard Montseny[3] Santiago Romaní[4]

1.Dept. of Software Engineering, University of Granada
Granada, Spain.
2.MAII Department, Technical University of Catalonia
Barcelona, Spain.
3.ESAII Department, Technical University of Catalonia
Barcelona, Spain.
4.Computer Engineering and Mathematics Department, Rovira I Virgili University
Tarragona, Spain.
Email: belenps@ugr.es, {pilar.sobrevilla,eduard.montseny}@upc.edu, santiago.romani@urv.net

Abstract— *Today many algorithms for monochrome images have been developed based on the information provided by the gradient vector. However, these algorithms can not be applied to color images without an accurate approximation of the color gradient vector argument. Moreover, there is a great number of applications that require to know with the maximum accuracy as possible the direction of the color variation in color images. This paper presents a new breakthrough in our work on the approximation of the argument of the color gradient vector. Taking into consideration that Hue and Saturation provide very useful basis for judging color uniformity, and that in the Smith's HSI color space there is a close relationship between chromaticity and how humans perceive colors, in our proposal the argument of the Chromaticity gradient vector is approached based on the Hue and Saturation information. Moreover, we present a fuzzy measure of the quality or reliability of the proposed approach that, considering the inherent vagueness of the chromaticity values of the image pixels, provides us with a credibility-accuracy degree of the obtained values.*

Keywords— Color gradient, Color image processing, Gradient argument, Gradient reliability, Gradient vector.

1 Introduction

Edge detection is one of the most important tasks in digital image processing and machine vision systems. Generally speaking, an edge implies the existence of abrupt changes or discontinuities in some visual property as light intensity, texture or color.

The advantage of color edge detection schemes over grayscale approaches is easily demonstrated by considering the fact that those edges that exist at the boundary between regions of different colors cannot be detected in grayscale images if there is no change in intensity. Among the existing approaches to detect color borders we can find active contour based methods [1], which use different approaches to perform the deformation process to dynamically adapt the active contour; multi-scale techniques [2], based on comparing the evolution of the borders through different scales; or morphological algorithms [3], that locate borders by computing the difference between a dilation and an erosion. However these methods just localize the maximum color variations or approach their magnitude, but not their direction.

A class of methods which not only localize the maximum color variations (edge localization) but also consider the direction of this variation (edge orientation) is the class of gradient based techniques.

The first methods proposed to compute the color gradient vector were mostly direct applications of the early intensity gradient methods. According to Lucchesse et al [4] these methods can be divided in those techniques that embed the variations of all color channels in a single measure [5, 6], and those that compute the gradient in each channel and then combine them according to certain criteria [7, 8]. A comprehensive analysis of color edge detectors can be found in [9].

Despite the importance and usefulness of the information provided by the argument of the gradient vector for many applications (texture characterization and analysis, 3D reconstruction, vehicle tracking and guidance,...), few techniques explicitly present and approach edge orientation. Among them we can find: proposals that approach the argument as the arc-tangent of the quotient between the vertical and horizontal partial derivatives [10]; Tensor based proposals [11] wherein the direction of the global color gradient is obtained from the tensor gradient components of multi-images regarded as vector fields; and Matrix based proposals [12] that approach the color gradient modulus as the highest eigenvalue in a given matrix, and its direction is given by the eigenvector associated to that eigenvalue.

The majority of the methods presented are focused on the RGB space. However, its lack of distinction between chromatic and achromatic information makes it unsuitable for obtaining edges in an image. A comparison of color edge detectors across several color spaces is presented in [13].

In this paper we present our ongoing work on the argument of the color gradient vector, focused on the Smith's HSI color space [14], which we began in [15]. In our proposal the argument of the *Chromaticity* gradient vector is approached based on the Hue and Saturation information, and we provide a fuzzy reliability degree of the obtained values for each edge pixel. This is quite useful, not only to evaluate the accuracy of our approach, but also to be used in applications that require to know the precision degree with which they are working. This is the case of astronomical images processing [16], the selection of optimal imaging planes in MRI [17] , or even the design of dichroic mirrors for LCDs [18]. In these applications

ISBN: 978-989-95079-6-8

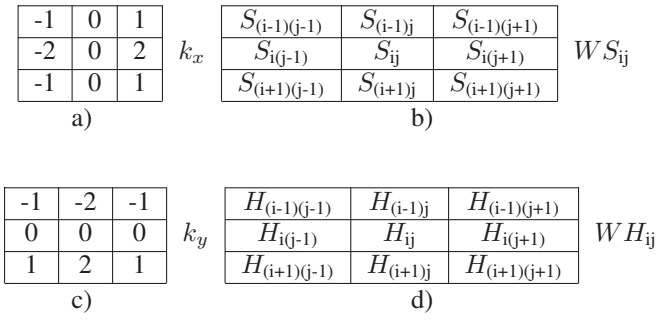

Figure 1: a) and c) Sobel Operators for the x and y directions, respectively. b) and d) 3x3 Saturation and Hue components windows of the source image, respectively.

an accurate contour extraction is necessary, and this is not possible without a good approach to the argument of the gradient vector, which also deals with the problems of imprecise contours.

Considering it, the paper is organized as follows. First, in section 2, we generalize the Sobel operators to compute the Hue and Saturation partial derivatives along the x and y directions. Then we present, in section 3, the way we combine the chromatic information to approach the partial derivatives; it will be used as directional components of the chromaticity gradient vector for approaching its argument. In section 4, we present the process and experiments carried out for obtaining a measure to evaluate the reliability of the color gradient vector argument approached. Finally we present some conclusions.

2 Proposed approximation of the Hue and Saturation partial derivatives

From the existing transformations to convert RGB components into perceptual ones, we have chosen Smith's model [14] based on its high independence between the three components, and its easier and faster calculation compared to other nonlinear models. This way we can consider color as a 1D+2D signal by decomposing it into its achromatic (I) and chromatic (H and S) components, what will provide us with a most useful basis for judging color uniformity.

In [15], having into consideration that Sobel masks (see Figure 1-a and 1-c) have slightly superior noise-suppression characteristics [13] than other operators, as Prewitt one, and that Sobel operator allows convolving separately the Hue and Saturation channels of the image, we presented an approximation to the partial derivatives of the chromatic color components extending this operator to approximate the variation of the Hue and Saturation components along the x and y directions.

2.1 Saturation First Order Derivatives

Given a pixel p_{ij} of the source image I, we will note by S_{ij} the magnitude of its Saturation, and WS_{ij} the window containing the Saturation values of the pixels falling into the 3x3 raster window centered at the pixel (see Figure 1-b).

Due to the fact that the areas of highest saturation gradient are where the saturation of the image changes rapidly over a few pixels, and are thus likely to represent edges, we can compute the Saturation partial derivatives, $\partial Sij/\partial x$ and $\partial Sij/\partial y$, by convolving kernels k_x and k_y with the WS_{ij} window , what provides us with the values given at equations (1) and (2).

2.2 Hue First Order Derivatives

Similarly to the Saturation case, we will note by H_{ij} the Hue magnitude of pixel p_{ij}, and WH_{ij} the window containing the Hue values of the pixels falling into the 3x3 raster window centered at that pixel (see Figure 1-d). However, while Euclidean distance is appropriate to compare the saturation values of two given colors, it is not the case of the Hue component. This is due to the ownership of Hue circularity, that is observed when this component is represented in a two-dimensional space. To overcome this problem, and consider the direction (the sign) of the difference between two Hue values we defined a Hue directed distance as follows:

Definition 2.1 *Let H_1 and H_2 be the hue values of pixels p_{i_1,j_1} and p_{i_2,j_2}, respectively. Then the* directed Hue distance *is defined as:*

$$\widehat{d}(H_1,H_2)=\begin{cases} H_2-H_1 & if\ \ |H_2-H_1|\leq 128 \\ H_2-H_1-255 & if\ \ H_2-H_1>128 \\ H_2-H_1+255 & if\ \ H_2-H_1<-128 \end{cases} \tag{3}$$

Then, convolution of kernels k_x and k_y are applied on the directed distances (3) obtained from the Hue values of WH_{ij}, instead of applying directly the Sobel operator over it.

As a result the Hue partial derivatives in both directions, $\partial Hij/\partial x$ and $\partial Hij/\partial y$, are given by equations (4) and (5).

3 Chromatic Gradient Vector Argument Approach

Once the Hue and Saturation partial derivatives have been approximated, next step consists in combining these values for obtaining the directional components of the *Chromatic Gradient Vector -CGV-*, or *Chromatic Partial Derivatives -CPD-*, which will be proportional to the directional components of the chromatic gradient vector, according to a given proportionality factor. In our case this problem has been figured out by mixing and merging previously obtained partial derivatives approximations according to next process.

1. First we consider two reference systems, one for the *x* direction, RS_x, and other for the *y* direction, RS_y, whose axes are the partial derivatives of *H* and *S* in the corresponding directions, ie: $RS_x=\{\partial H/\partial x, \partial S/\partial x\}$ and $RS_y=\{\partial H/\partial y, \partial S/\partial y\}$. On these systems we represent the values of the approaches obtained at the previous step, what provides us with two chromaticity vectors, one in the *x* direction, $\overrightarrow{Chr_{ij}x}=(\partial H_{ij}/\partial x, \partial S_{ij}/\partial x)$, and other in the *y* direction, $\overrightarrow{Chr_{ij}y}=(\partial H_{ij}/\partial y, \partial S_{ij}/\partial y)$ (line-dot vectors of Figure 2-a and 2-b). We also obtain de modules of these vectors, $\|\overrightarrow{Chr_{ij}x}\|$ and $\|\overrightarrow{Chr_{ij}y}\|$, which we call the *Directional Chromaticity Variations*.

2. Because the vectors obtained are represented into two different reference systems, to be able to mix and merge the information they contain is necessary to get a reference system wherein both vectors can be represented.

ISBN: 978-989-95079-6-8

$$\partial S_{ij}/\partial x = \frac{k_x * WS_{ij}}{8} = \frac{(S_{(i-1)(j+1)} - S_{(i-1)(j-1)}) + 2(S_{(i)(j+1)} - S_{(i)(j-1)}) + (S_{(i+1)(j+1)} - S_{(i+1)(j-1)})}{8} \quad (1)$$

$$\partial S_{ij}/\partial y = \frac{k_y * WS_{ij}}{8} = \frac{(S_{(i+1)(j-1)} - S_{(i-1)(j-1)}) + 2(S_{(i+1)(j)} - S_{(i-1)(j)}) + (S_{(i+1)(j+1)} - S_{(i-1)(j+1)})}{8} \quad (2)$$

$$\partial H_{ij}/\partial x = \frac{\widehat{d}(H_{(i-1)(j+1)}, H_{(i-1)(j-1)}) + 2\widehat{d}(H_{(i)(j+1)}, H_{(i)(j-1)}) + \widehat{d}(H_{(i+1)(j+1)}H_{(i+1)(j-1)})}{8} \quad (4)$$

$$\partial H_{ij}/\partial y = \frac{\widehat{d}(H_{(i+1)(j-1)}, H_{(i-1)(j-1)}) + 2\widehat{d}(H_{(i+1)(j)}, H_{(i-1)(j)}) + \widehat{d}(H_{(i+1)(j+1)}H_{(i-1)(j+1)})}{8} \quad (5)$$

To do it, due to axes $\partial H/\partial x = \partial S/\partial x$ and $\partial H/\partial y = \partial S/\partial y$ point to the higher potentials of *H* and *S*, and that both components grow equally within these axes, our proposal is to project the chromaticity vectors into them. So, our approach to the above mentioned *CPD* vectors, $\overrightarrow{\partial C_{ij}/\partial x}$ and $\overrightarrow{\partial C_{ij}/\partial y}$, is given by equations (6) and (7), where $\overrightarrow{u} = (\cos(45^o), \sin(45^o))$. These new vectors, that appear as dotted arrows in Figures 2-a and 2-b, will be used at next section to approach of the *CGVA*.

$$\overrightarrow{\partial C_{ij}/\partial x} = proj_{\overrightarrow{u}}\overrightarrow{Chr_{ij}x} \quad (6)$$

$$\overrightarrow{\partial C_{ij}/\partial y} = proj_{\overrightarrow{u}}\overrightarrow{Chr_{ij}y} \quad (7)$$

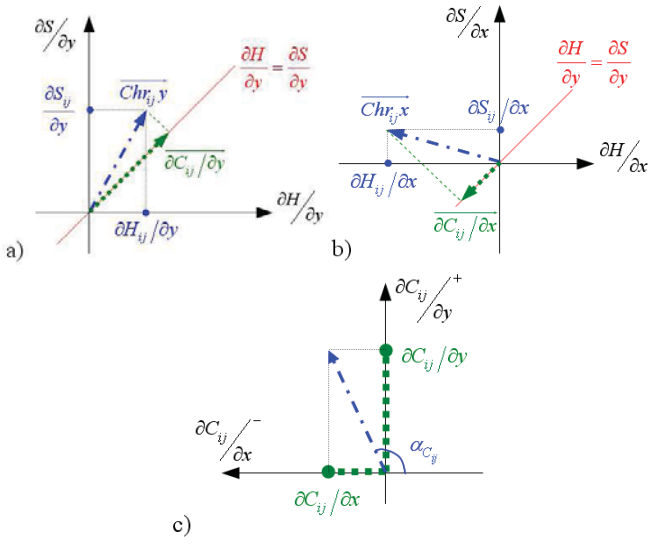

Figure 2: a, b: Calculation of the *CPD* vectors in each direction. c: Approach to the *CGVA*.

3. Applying the usual calculation of a projection, as we are interested in considering the argument of the *CPD* vectors, but considering their direction, the components of the *CGVA* approach are given using the scalar product, as depicted by equations (8) and (9).

$$\partial C_{ij}/\partial x = (\partial H_{ij}/\partial x, \partial S_{ij}/\partial x) \cdot (\sqrt{2}/2, \sqrt{2}/2) \quad (8)$$

$$\partial C_{ij}/\partial y = (\partial H_{ij}/\partial y, \partial S_{ij}/\partial y) \cdot (\sqrt{2}/2, \sqrt{2}/2) \quad (9)$$

Then, translating these values to the coordinate system of axes $\partial C_{ij}/\partial x$ and $\partial C_{ij}/\partial y$ we get the approach to the *Chromatic Gradient Vector*, and the argument of this vector, $\alpha_{C_{ij}} = \arctan(\frac{\partial C_{ij}/\partial y}{\partial C_{ij}/\partial x})$, provides us with the *CGVA* approach, as represented by Figure 2-c. This argument provides us with a direction that is perpendicular to the contour and so it is 0 for a vertical edge and increases for edges moving anti-clockwise of it.

4 Reliability degree of the color gradient argument approach

To assess the performance (goodness) of the proposed approach, we have defined a measure of reliability that must consider the sources of uncertainty of the factors having influence on the results obtained when the approach is applied on an image. So, for obtaining the reliability measure we have developed a set of experiments that allow us to study the relationship among: the error given by the approach with regard to the actual value of the argument, the *Chromatic Partial Derivatives*, and the *Directional Chromaticity Variations*. To carry out our experiments we have designed a set of images as explained in the next section.

4.1 *Obtaining the set of synthetic images*

To perform our experiments we built a set of images, consisting of a square with a circle in the center. The process for obtaining the images has been carried out as follows:

1. First, after dividing the RGB cube into 512 boxels, we select a point of each one of the boxes, so obtaining a set of 512 colors distributed almost homogeneously.

2. Then we generated a set of images using all the possible combinations of colors for background and foreground. For each image if a pixel is completely included in the background or in the circle, it is assigned the corresponding color. If the pixel belongs to background and foreground, after evaluating the area of the pixel belonging to each region, we assign to the pixel a color that is the weighted average of the two colors.

3. Finally, after smoothing the images using a 3x3 window to create a gradient in the boundary of the circles, the transformation from RGB to HSI is carried out.

4.2 *Experimental design*

For all the pixels in the borders of the circumferences, we have computed the argument of the *Chromaticity Gradient Vector* using the proposed approach. Since we know the position of the point and the center of the circle, we know the real value of the argument for each border pixel ($\arg_{ij}$). Having both

ISBN: 978-989-95079-6-8

values we can accurately evaluate the error at pixel (i, j) as $E^{ij} = |\arg_{ij} - \arg \alpha_{C_{ij}}|$.

In our experiments for obtaining the reliability degree we have studied the relationship among the aforementioned error, the *Directional Chromaticity Variations* ($\|\overrightarrow{Chr_{ij}x}\|$, and $\|\overrightarrow{Chr_{ij}y}\|$), and the smaller angles of the *Chromaticity Vectors* ($\overrightarrow{Chr_{ij}x}$, and $\overrightarrow{Chr_{ij}y}$) with the lines $\partial S/\partial x = -\partial H/\partial x$ and $\partial S/\partial y = -\partial H/\partial y$. These angles are given by:

$$E(\alpha_x^{ij}) = \begin{cases} |\arg \alpha_x^{ij} - 135| & \text{if } 45 < \arg \alpha_x^{ij} < 225 \\ |\arg \alpha_x^{ij} - 315| & else \end{cases} \quad (10)$$

$$E(\alpha_y^{ij}) = \begin{cases} |\arg \alpha_y^{ij} - 135| & \text{if } 45 < \arg \alpha_y^{ij} < 225 \\ |\arg \alpha_y^{ij} - 315| & else \end{cases} \quad (11)$$

Where α_x^{ij} and α_y^{ij} are the angles of the vectors $\overrightarrow{Chr_{ij}x}$ and $\overrightarrow{Chr_{ij}y}$ with the lines $\partial S/\partial x = \partial H/\partial x$ and $\partial S/\partial y = \partial H/\partial y$, respectively.

For each pixel (i, j) in the border of the circles we have obtained the values of E^{ij}, $\|\overrightarrow{Chr_{ij}x}\|$, $\|\overrightarrow{Chr_{ij}y}\|$, $E(\alpha_x^{ij})$, and $E(\alpha_y^{ij})$. Then we have analyzed and discussed the relationship between the average error and the values obtained for the four parameters considered by pairs.

4.3 Experimental analysis

For analyzing the obtained results we have represented in $3-D$ graphics the error values E^{ij} for each point (i, j) of the planes: $(E(\alpha_x^{ij}), E(\alpha_y^{ij}))$, $(\|\overrightarrow{Chr_{ij}x}\|, \|\overrightarrow{Chr_{ij}y}\|)$, and the planes $(\|\overrightarrow{Chr_{ij}x}\|, E(\alpha_x^{ij}))$, $(\|\overrightarrow{Chr_{ij}x}\|, E(\alpha_y^{ij}))$, $(\|\overrightarrow{Chr_{ij}y}\|, E(\alpha_y^{ij}))$, and $(\|\overrightarrow{Chr_{ij}y}\|, E(\alpha_x^{ij}))$. In these representations the gray level is proportional to the value of the average error for each point. So, the higher the gray level the lowest the error is.

As can be observed at the left image of Figure 3, when we consider the differences of the arguments, the values of the errors are small or large, and errors distribution indicates a great dependency among the error and the values of $E(\alpha_x^{ij})$, $E(\alpha_y^{ij})$.

When we consider the values of the *Directional Chromaticity Variations* (right image of Figure 3) the values of the errors are small and medium. However, the relationship among the error values and those of the parameters is very small, what is due to for almost each pair $(\|\overrightarrow{Chr_{ij}x}\|, \|\overrightarrow{Chr_{ij}y}\|)$ the errors are small.

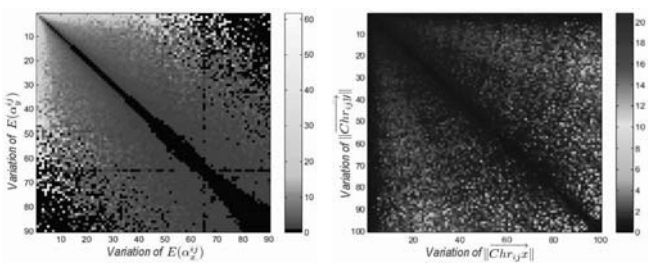

Figure 3: Representation of error magnitude for $E(\alpha_x^{ij})$ vs $E(\alpha_y^{ij})$ in the left image, and for $\|\overrightarrow{Chr_{ij}x}\|$ vs $\|\overrightarrow{Chr_{ij}y}\|$ in the right image.

In the case of the plane $(\|\overrightarrow{Chr_{ij}y}\|, E(\alpha_x^{ij}))$, and similarly for $(\|\overrightarrow{Chr_{ij}x}\|, E(\alpha_y^{ij}))$, the errors are mainly small. The medium and large errors that occur are highly concentrated, leaving almost the entire plane to the small errors (see left image of Figure 4), what implies a correlation among the error and the values of the parameters.

Finally, having a look at right image of Figure 4 it can be observed that in the case of the plane $(\|\overrightarrow{Chr_{ij}y}\|, E(\alpha_y^{ij}))$ appear small and big error values. In this case, while small errors are highly concentrated large errors are widely distributed, which indicates a certain relation between the error and the parameter values. A similar behavior is observed in the case of the plane $(\|\overrightarrow{Chr_{ij}x}\|, E(\alpha_x^{ij}))$

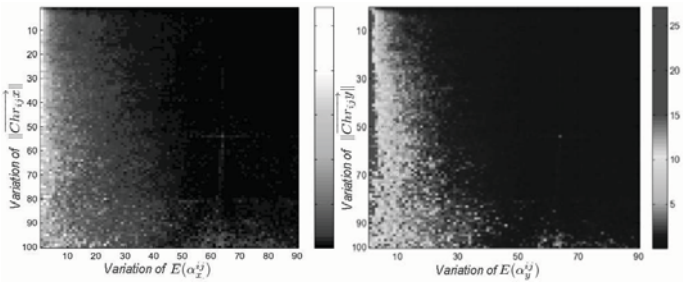

Figure 4: Left image represents the error magnitude for $\|\overrightarrow{Chr_{ij}^{x}}\|$ vs $E(\alpha_x^{ij})$.Right image represents the error magnitude for $\|\overrightarrow{Chr_{ij}^{y}}\|$ vs $E(\alpha_y^{ij})$.

As a consequence of previous analysis it can be deduced that the most important information for obtaining the reliability of the proposed approach is given by considering the values of $E(\alpha_x^{ij})$ vs $E(\alpha_y^{ij})$, and the less relevant information is provided by the values of $\|\overrightarrow{Chr_{ij}x}\|$ vs $\|\overrightarrow{Chr_{ij}y}\|$. On the other hand some information is provided when we consider the pairs $(E(\alpha_x^{ij}), \|\overrightarrow{Chr_{ij}y}\|)$ and $(E(\alpha_x^{ij}), \|\overrightarrow{Chr_{ij}x}\|)$.

4.4 Experimental results and Reliability degree

Based on the results obtained at previous step, we have considered the *Reliability Labels*: $Great$ (G), $Medium$ (M), $Small$ (S), and *Very Small* (VS). Then a reliability degree has been associated to each point of the considered plains, according to the error at each point, by means of the membership functions depicted at Figure 5.

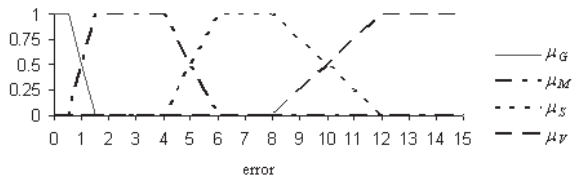

Figure 5: Reliability membership functions.

These membership functions have been obtained through a heuristic analysis of the results. The border values between each of the two central functions have been selected so that the error value of the 75%, the 85% and the 90% of the pixels are lower than such value.

The graphs obtained for each one of the cases considered at the previous step leads to the appearance of some lines. For each case, these lines act as boundaries between the different reliability degrees of the points in the corresponding plain.

ISBN: 978-989-95079-6-8

So, these lines will allow us to obtain the *Reliability Functions* of the proposed approach. Due to lack of space here only present the results obtained for the case of the $E(\alpha_x^{ij})$ vs $E(\alpha_y^{ij})$. For this case Figure 6 depicts the result of using the reliability degrees. Having a look at this image is it clear that appear some lines delimiting the different reliability regions, from $Great$ (dark grey level) to *Very Small* (very clear grey level). The lines obtained in this case are given by equations (12) to (22). Afterwards, these lines are used for obtaining the corresponding *Reliability Degrees* that, in this case are depicted by equations (23) to (26).

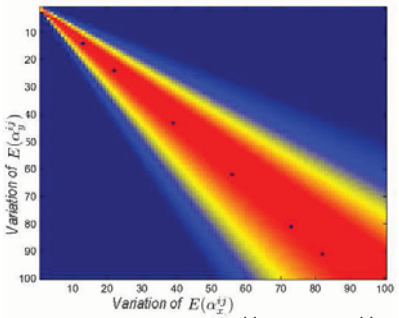

Figure 6: Graph obtained for $E(\alpha_x^{ij})$ vs $E(\alpha_y^{ij})$ using the reliability membership functions.

$$r_0(i,j) : E_x^{ij} = E_y^{ij} \tag{12}$$

$$r_1(i,j) : 25 \cdot E_x^{ij} - 27,5 \cdot E_y^{ij} + 6 = 0 \tag{13}$$

$$r_2(i,j) : 16 \cdot E_x^{ij} - 29 \cdot E_y^{ij} + 13 = 0 \tag{14}$$

$$r_3(i,j) : 10,6 \cdot E_x^{ij} - 29,1 \cdot E_y^{ij} + 16,65 = 0 \tag{15}$$

$$r_4(i,j) : 4,75 \cdot E_x^{ij} - 29,25 \cdot E_y^{ij} + 18,375 = 0 \tag{16}$$

$$r_5(i,j) : 2,5 \cdot E_x^{ij} - 29,5 \cdot E_y^{ij} + 13,5 = 0 \tag{17}$$

$$r_6(i,j) : 27,5 \cdot E_x^{ij} - 25 \cdot E_y^{ij} - 6 = 0 \tag{18}$$

$$r_7(i,j) : 29 \cdot E_x^{ij} - 16 \cdot E_y^{ij} - 13 = 0 \tag{19}$$

$$r_8(i,j) : 29,1 \cdot E_x^{ij} - 10,6 \cdot E_y^{ij} - 16,65 = 0 \tag{20}$$

$$r_9(i,j) : 29,25 \cdot E_x^{ij} - 4,75 \cdot E_y^{ij} - 18,375 = 0 \tag{21}$$

$$r_{10}(i,j) : 29,5 \cdot E_x^{ij} - 2,5 \cdot E_y^{ij} - 13,5 = 0 \tag{22}$$

Finally, for obtaining the *Reliability Degree* of the *Chromatic Gradient Vector Argument Approach* value for each point, the previous reliabilities for each case has to be aggregated. To do it, considering that all the individual values have influence in the final reliability degree, we can consider a *T-Norm* to perform the aggregation. Among the great variety of available *T-Norm* we propose to use the *Minimum* due to: its simplicity, fast computation, and that it is the greatest *T-Norm*.

5 Conclusions

In this paper we have presented an approach of the chromatic component for the argument of the gradient vector. After computing the hue and saturation partial derivatives on each direction, this information has been merged and combined through projections for obtaining the directional components of the chromaticity gradient vector used to approach the argument.

We have also presented a study of the error variability produced by the proposed approach with regard to the four main parameters used within the proposed approach. This will allow us to improve the approximation, as well as obtaining an approach for the module of the gradient vector.

A very important point to highlight is that, as a result of the analysis of the error variability, we obtained a value that provides the credibility of the value provided by the approximation. This is very important because it will allow to use the value of the gradient vector argument for each point knowing its reliability degree.

Acknowledgment

This paper has been partially supported by the projects P07-TIC-03175, P06-TIC-01570 and TIN2007-68063.

References

[1] A. Maalouf, A. Maalouf, P. Carre, B. Augereau, and C. Fernandez-Maloigne. Foveal wavelet-based color active contour. In P. Carre, editor, *Image Processing, 2007. ICIP 2007. IEEE Int. Conf. on*, volume 1, pages I – 245–I – 248, 2007.

[2] I. Vanhamel, I. Vanhamel, I. Pratikakis, and H. Sahli. Multiscale gradient watersheds of color images. *Image Processing, IEEE Transactions on*, 12(6):617–626, 2003.

[3] A.N. Evans and A.N. Evans. Morphological gradient operators for colour images. In *Image Processing, 2004. ICIP '04. 2004 Int. Conf. on*, volume 5, pages 3089–3092 Vol. 5, 2004.

[4] L. Lucchese and S. K. Mitra. Color image segmentation: A state-of-art survey. In *Proc. Indian Nat. Sci. Acad. (INSA-A)*, volume 67-A, pages 207–221, 2001.

[5] M. Chapron. A color edge detector based on statistical rupture tests. In *Image Processing, 2000. Proc. 2000 Int. Conf. on*, volume 2, pages 820–823 vol.2, 2000.

[6] M. A. Ruzon and C. Tomasi. Color edge detection with the compass operator. *Proc. IEEE Conf. Computer Vision and Pattern Recognition.*, 2:160–166, 1999.

[7] M. Heddley. Segmentation of color images using spatial and color space information. *J. Electron. Imag.*, 1(4):374–380, 1992.

[8] Jianping Fan, Jianping Fan, D.K.Y. Yau, A.K. Elmagarmid, and W.G. Aref. Automatic image segmentation by integrating color-edge extraction and seeded region growing. *Image Processing, IEEE Transactions on*, 10(10):1454–1466, 2001.

[9] A. Koschan and M. Abidi. Detection and classification of edges in color images. *Signal Processing Magazine, IEEE*, 22(1):64–73, 2005.

[10] T. Carron and P. Lambert. Color edge detector using jointly hue, saturation and intensity. In *Image Processing, 1994. Proc. ICIP-94., IEEE Int. Conf.*, volume 3, pages 977–981, 1994.

[11] Silvano Di Zenzo. A note on the gradient of a multi-image. *Computer Vision, Graphics, and Image Processing*, 33(1):116–125, 1986.

[12] Anwander-A, Neyran-B, and Baskurt-A. Multiscale color gradient for image segmentation. *Traitement du Signal*, 18(2):129–42, 2001.

[13] S. Wesolkowski, S. Wesolkowski, M.E. Jernigan, and R.D. Dony. Comparison of color image edge detectors in multiple color spaces. In M.E. Jernigan, editor, *Image Processing, 2000. Proc. 2000 Int. Conf. on*, volume 2, pages 796–799 vol.2, 2000.

ISBN: 978-989-95079-6-8

$$\mu_G(E_x^{ij},E_y^{ij})=\begin{cases}0 & \text{if } r_8(i,j)<0 \text{ or } r_2(i,j)>0\\ 1 & \text{if } r_6(i,j)>0 \text{ and } r_1(i,j)<0\\ \dfrac{d((E_x^{ij},E_y^{ij}),r_7(i,j))}{d((E_x^{ij},E_y^{ij}),r_7^{ij})+d((E_x^{ij},E_y^{ij}),r_6(i,j))} & \text{if } r_6(i,j)<0 \text{ and } r_7(i,j)>0\\ \dfrac{d((E_x^{ij},E_y^{ij}),r_2(i,j))}{d((E_x^{ij},E_y^{ij}),r_2^{ij})+d((E_x^{ij},E_y^{ij}),r_1(i,j))} & \text{else}\end{cases} \tag{23}$$

$$\mu_M(E_x^{ij},E_y^{ij})=\begin{cases}0 & \text{if } r_8(i,j)<0 \text{ or } r_3(i,j)>0\\ 1 & \text{if } (r_6(i,j)<0 \text{ and } r_7(i,j)>0)\\ & \textit{or } (r_1(i,j)>0 \text{ and } r_2(i,j)<0)\\ \dfrac{d((E_x^{ij},E_y^{ij}),r_0(i,j))}{d((E_x^{ij},E_y^{ij}),r_0^{ij})+d((E_x^{ij},E_y^{ij}),r_6(i,j))} & \text{if } r_0(i,j)>0 \text{ and } r_6(i,j)<0\\ \dfrac{d((E_x^{ij},E_y^{ij}),r_0(i,j))}{d((E_x^{ij},E_y^{ij}),r_0^{ij})+d((E_x^{ij},E_y^{ij}),r_1(i,j))} & \text{if } r_0(i,j)<0 \text{ and } r_1(i,j)>0\\ \dfrac{d((E_x^{ij},E_y^{ij}),r_8(i,j))}{d((E_x^{ij},E_y^{ij}),r_8^{ij})+d((E_x^{ij},E_y^{ij}),r_7(i,j))} & \text{if } r_7(i,j)<0 \text{ and } r_8(i,j)>0\\ \dfrac{d((E_x^{ij},E_y^{ij}),r_3(i,j))}{d((E_x^{ij},E_y^{ij}),r_3^{ij})+d((E_x^{ij},E_y^{ij}),r_2(i,j))} & \text{else}\end{cases} \tag{24}$$

$$\mu_S(E_x^{ij},E_y^{ij})=\begin{cases}0 & \text{if } (r_{10}(i,j)<0 \text{ or } r_5(i,j)>0)\\ & \textit{or } (r_7(i,j)>0 \text{ and } r_2(i,j)<0)\\ 1 & \text{if } (r_8(i,j)<0 \text{ and } r_9(i,j)>0)\\ & \textit{or } (r_3(i,j)>0 \text{ and } r_4(i,j)<0)\\ \dfrac{d((E_x^{ij},E_y^{ij}),r_7(i,j))}{d((E_x^{ij},E_y^{ij}),r_7^{ij})+d((E_x^{ij},E_y^{ij}),r_8(i,j))} & \text{if } r_7(i,j)<0 \text{ and } r_8(i,j)>0\\ \dfrac{d((E_x^{ij},E_y^{ij}),r_2(i,j))}{d((E_x^{ij},E_y^{ij}),r_2^{ij})+d((E_x^{ij},E_y^{ij}),r_3(i,j))} & \text{if } r_2(i,j)>0 \text{ and } r_3(i,j)<0\\ \dfrac{d((E_x^{ij},E_y^{ij}),r_{10}(i,j))}{d((E_x^{ij},E_y^{ij}),r_{10}^{ij})+d((E_x^{ij},E_y^{ij}),r_9(i,j))} & \text{if } r_9(i,j)<0 \text{ and } r_{10}(i,j)>0\\ \dfrac{d((E_x^{ij},E_y^{ij}),r_5(i,j))}{d((E_x^{ij},E_y^{ij}),r_5^{ij})+d((E_x^{ij},E_y^{ij}),r_4(i,j))} & \text{else}\end{cases} \tag{25}$$

$$\mu_{VS}(E_x^{ij},E_y^{ij})=\begin{cases}0 & \text{if } r_9(i,j)>0 \text{ and } r_4(i,j)><0\\ 1 & \text{if } r_{10}(i,j)>0 \text{ and } r_5(i,j)<0\\ \dfrac{d((E_x^{ij},E_y^{ij}),r_9(i,j))}{d((E_x^{ij},E_y^{ij}),r_9^{ij})+d((E_x^{ij},E_y^{ij}),r_{810}(i,j))} & \text{if } r_9(i,j)<0 \text{ and } r_{10}(i,j)>0\\ \dfrac{d((E_x^{ij},E_y^{ij}),r_4(i,j))}{d((E_x^{ij},E_y^{ij}),r_4^{ij})+d((E_x^{ij},E_y^{ij}),r_5(i,j))} & \text{else}\end{cases} \tag{26}$$

[14] A.R. Smith. Color gamut transform pairs. *Computer Graphics*, 12:12–19, 1978.

[15] P. Sobrevilla B. Prados-Suarez, E. Montseny and S. Romanís. An approach to color gradient vector argument considering data uncertainty. *in Procc Joint Eusflat-LFA Conf.*, 2:705–708, 2000.

[16] Changbom-Park and Yun-Young-Choi. Morphology segregation of galaxies in color-color gradient space. *Astrophysical Journal, Letters*, 635(1):L29–32, 2005.

[17] Levine RA Okada RD Brady TJ. Dinsmore RE, Wismer GL. Magnetic resonance imaging of the heart: positioning and gradient angle selection for optimal imaging planes. *American journal of roentgenology, radium therapy and nuclear medicine.*, 143(6):1135–42, 1984.

[18] GU P. GUAN A. LU W., ZHENG Z. Gradient angle design of dichroic mirrors used in lcd projection display. In *Proc Int Disp Workshops*, volume 11, pages 1697–1699, 2004.

ISBN: 978-989-95079-6-8